

Energetic Protons and Deuterons Emitted Following μ^- Capture by ^3He Nuclei

W. J. Cummings,⁽¹⁾ G. E. Dodge,⁽¹⁾ S. S. Hanna,⁽¹⁾ B. H. King,⁽¹⁾ S. E. Kuhn,^{(1),(a)} Y. M. Shin,⁽²⁾
 R. Helmer,⁽³⁾ R. B. Schubank,⁽³⁾ N. R. Stevenson,⁽³⁾ U. Wienands,⁽³⁾ Y. K. Lee,⁽⁴⁾ G. R. Mason,⁽⁵⁾
 B. E. King,⁽⁶⁾ K. S. Chung,⁽⁷⁾ J. M. Lee,⁽⁷⁾ and D. P. Rosenzweig⁽⁸⁾

⁽¹⁾Stanford University, Stanford, California 94305

⁽²⁾University of Saskatchewan, Saskatoon, Saskatchewan, Canada S7N 0W0

⁽³⁾TRIUMF, Vancouver, British Columbia, Canada V6T 2A3

⁽⁴⁾The Johns Hopkins University, Baltimore, Maryland 21218

⁽⁵⁾University of Victoria, Victoria, British Columbia, Canada V8W 3P6

⁽⁶⁾Simon Fraser University, Burnaby, British Columbia, Canada V5A 1S6

⁽⁷⁾Yonsei University, Seoul 120-749, Korea

⁽⁸⁾University of Washington, Seattle, Washington 98195

(Received 7 October 1991)

Spectra of energetic protons and deuterons emitted following negative muon capture from rest in ^3He have been measured for the first time. Significant capture strength is observed at high energy transfers ($m_\mu - E_\nu > 60$ MeV) for the two-body and three-body breakup channels, indicative of the importance of nucleon-nucleon correlations and meson exchange currents in the capture process. A simple plane wave impulse approximation calculation reproduces the proton spectrum reasonably well, but underpredicts the deuteron rate at the highest energies by a large factor.

PACS numbers: 23.40.Hc, 25.10.+s, 27.10.+h

Total capture rates for nuclear muon capture have been extensively studied for many years [1,2]. Early investigations studied the hadronic form factors of the weak interaction and verified the universality of the $V-A$ nature of the weak current [3]. Other investigations led to the use of nuclear muon capture rates as a probe of the nuclear structure [4]. The availability of high-quality intense muon beams from meson factories has allowed investigations of exclusive channels in nuclear muon capture [5]. These studies showed that a significant fraction of muon captures in nuclei led to nuclear excitations above 35 MeV [6,7]. This result is unexpected in a one-body impulse approximation based on Fermi-gas or shell-model wave functions for the nucleon momentum distribution [3,8]. Capture mechanisms involving two or more nucleons, similar to pion capture processes, were proposed to explain this strength at large energy transfer [6-8]. Ultimately, one would want to predict the particle emission spectrum using a realistic many-body wave function with high-momentum components, nucleon-nucleon correlations, and a correct treatment of meson exchange currents (MEC). Unfortunately, most experiments were performed in complex nuclei where complete microscopic theoretical treatments are extremely difficult. Therefore, very recent theoretical [9,10] and experimental [11] investigations have concentrated on the simplest nuclear system, the deuteron. A measurement of the neutron energy spectrum at the highest energies following negative muon capture by deuterium [11] showed an indication of an enhancement near the end point. This enhancement had been theoretically predicted [10] in a calculation which found that the inclusion of MEC triples the capture rate near the end point ($E_\nu=0$). Unfortunately, the limited statistics and large background uncertainty in Ref. [11] made the results inconclusive.

Recently, there has been considerable progress towards obtaining an exact microscopic treatment of the three-nucleon wave function [12]. This work has opened up the possibility of performing detailed calculations of μ^- capture in the $A=3$ system and studying the relative importance of high-momentum components in the wave function and of meson-exchange-current contributions to the weak capture interaction. Therefore, the present work was undertaken to study muon capture at large energy transfer in ^3He . The advantage of studying μ^- capture by a nucleus with $Z > 1$ is the emission of charged fragments which allows experimental detection with high efficiency and good background suppression. There are three reaction channels for the capture of a negative muon on ^3He :

$$\mu^- + ^3\text{He} \rightarrow t + \nu_\mu, \quad (1)$$

$$\mu^- + ^3\text{He} \rightarrow d + n + \nu_\mu, \quad (2)$$

$$\mu^- + ^3\text{He} \rightarrow p + n + n + \nu_\mu. \quad (3)$$

The energy transfer in reaction (1) is small because of the kinematics of the two-body final state. The study of muon capture at large energy transfer requires measuring the energy spectra of the highest energy protons and deuterons produced by reactions (2) and (3).

The experiment was performed at the Tri-University Meson Facility (TRIUMF) in Vancouver, British Columbia (Canada) at the superconducting muon channel (M9B). The experimental apparatus is shown in Fig. 1. Negative muons were stopped inside a cylindrical target cell filled with ^3He gas at a temperature of 4.2 K and a pressure of 1 atm (target density of 11 mg/cm³). The interior wall of the cell was lined with lead foil. Muon stops in the target were identified by signals in the

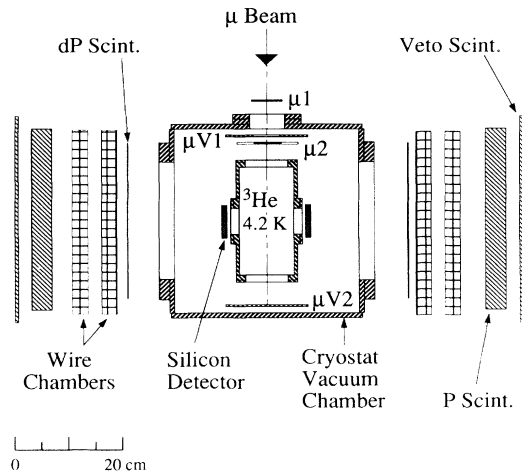


FIG. 1. The experimental arrangement. Shown are the two identical charged-particle detection systems on either side of the ^3He gas cell in which the muons are stopped.

upstream beam counters ($\mu 1$ and $\mu 2$), no signal in the upstream veto counter ($\mu V1$) which had a 5-cm circular hole in the center, and no signal in the downstream veto counter ($\mu V2$). The pion contamination of the beam was less than 0.05%, and the fraction of electrons in the beam was about 20%.

Charged particles exited the target cell through 5-cm-diam windows (12.5- μm Havar) and were measured in either of two symmetric detector telescopes, extending out from each of the windows as shown in Fig. 1. The first element of each telescope was a 240- μm -thick 4.4-cm-diam silicon surface barrier detector (Si) located just outside the target exit window and operated at a temperature of 77 K. This detector recorded charged particles originating in the target and measured their energy loss for particle identification. After exiting the cryostat vacuum chamber, the particles entered a 1-mm-thick plastic scintillator (BC 408) detector (dP). Deuterons with initial energies between 15 and 23 MeV stopped in this detector. The highest energy deuterons and protons passed through the dP detector, thus providing an additional energy-loss measurement for particle identification. These high energy charged particles were then detected by a pair of delay-line wire chambers in order to verify that they originated in the target and to measure their angular distribution. They were finally stopped in a 36-mm-thick plastic scintillator (BC 408) detector (P). An additional 5-mm-thick plastic scintillator detector (Veto) was located behind the P detector to identify penetrating particles (electrons).

Monoenergetic deuterons (45 MeV) and protons with energies up to 90 MeV from negative pion capture on ^3He were used to calibrate the charged-particle detectors. For this purpose, the beam line was periodically tuned to allow pions to stop in the target. In addition, the detector

signals from muon decay electrons were used to monitor continuously the detector calibrations.

Events were recorded on tape if they contained a signal in the dP detector in coincidence with either the Si or P detector. In addition, these events were required to occur within a gate that was open from 0.3 to 4.5 μs after a valid muon stop. Events which occurred in "prompt" coincidence with any beam particle entering the target (signal in $\mu 1$, $\mu 2$, or $\mu V1$) were rejected in order to suppress pion-induced events. Events were also removed from the data sample if a second muon entered the target (during the open gate) before the charged particle was emitted. The surviving events were separated into four types. Penetrating particles with signals in all scintillator detectors were identified as Michel electrons from muon decay and were prescaled by a factor of 100. High energy hadronic events were identified by observing a signal in the P detector and separated into proton and deuteron events using the energy-loss information from the Si and dP detectors, as well as measurements of the time of flight from dP to P. Lower energy deuterons which stopped in the left dP detector (as seen by the beam) were identified using a two-dimensional gate based on energy loss in the Si detector and energy deposited in the dP detector. As a result of differences in Si and dP detector performances, only the left detector arm had sufficient energy resolution to allow a clean identification of these lower energy deuterons.

Events of all four types were checked to see that they had the correct lifetime. The time between the arrival of the muon and the charged-particle detection was measured for each event. The time distribution obtained was analyzed using a maximum-likelihood analysis. The decay electron lifetime determined by this method ($2.11 \pm 0.02 \mu\text{s}$) agrees well with the expected lifetime of 2.13 μs . The proton and deuteron results also agree with the 2.13- μs lifetime within statistical errors of $\pm 0.2 \mu\text{s}$, with one exception. The left-side hadronic events which stop in P show evidence for a 30% background contamination, random in time. This background could be attributed to protons produced by penetrating high energy neutrons emitted from the meson production target. Because of the arrangement of the experiment relative to the primary beam line, this background created no problem for the right detector arm. The contamination in the left-side events was eliminated by subtracting the P pulse-height spectrum for events which occurred in the second half of the muon gate from those that occurred in the first half, at the expense of a considerable increase in the statistical error for that side.

A Monte Carlo simulation of the entire experimental setup was used to determine the geometrical acceptance and detection efficiency of the charged-particle telescopes as well as the fraction of muons which stopped in the fiducial region of the target cell. The stopping distribution in the gas cell was determined by simulating the scattering of the beam particles as they slow down. All

relevant beam properties were measured and used as input to this simulation. The stopped muon distribution was then used to simulate the emission of charged particles following muon capture. Extensive comparisons of energy spectra in all detectors from both decay electron events and events from stopped pions with Monte Carlo-generated events show good agreement between the measured and the predicted shapes. The detection efficiency for protons was found to be $\approx 90\%$ and independent of energy above a threshold of ≈ 20 MeV. The acceptance of each detector telescope was dominated by the acceptance of its Si detector and in each case was $\approx 0.7\%$. The overall normalization of the data was determined using this technique to an accuracy of $\pm 10\%$.

The energy spectrum of the high energy protons expressed in terms of partial muon capture rates in ${}^3\text{He}$ is shown in Fig. 2. The circular data points correspond to events in the right detector telescope, while the triangular points with the much larger error bars are the background-subtracted results from the left detector telescope. The two data sets are consistent within the quality of the data. In both cases the error bars are representative of the statistical error only and do not include the $\approx 10\%$ error in the normalization. We performed a simple plane wave impulse approximation (PWIA) calculation for reaction (3) and show the result as the solid curve in Fig. 2. For this calculation, we used the bound proton spectral function $S(E, p)$ for ${}^3\text{He}$ derived from a measurement of ${}^3\text{He}(e, e'p)$ [13], and the standard Hamiltonian for μ^- capture by the proton [3]. We then assumed that the spectator pn pair (with internal energy $E - Q$) decays iso-

tropically, leading to the observed proton. Both the data points and the calculated curve are averaged over 5-MeV-wide energy bins. This calculation is in fair agreement with our data.

The deuteron results are shown in Fig. 3. Because of the narrow energy acceptance for deuterons in our detectors, there are only three data points. The highest energy points are extracted from deuterons which stop in the P detectors. The other point is extracted from deuterons stopping in the left dP detector only. Again the vertical error bars shown are statistical only. The horizontal error bars show the uncertainty in the centroid of the range of initial deuteron energies which contribute to each data point. The solid curve shown in Fig. 3 is the result of a PWIA calculation similar to the calculation mentioned above. This calculation underpredicts the data by a factor of 2 to 6.

The relatively good agreement between our simple model calculation and the proton data is partially fortuitous. Proper inclusion of final-state interactions and use of realistic three-body wave functions could alter that picture substantially. On the other hand, the deuteron calculation should be at least as reliable as the proton calculation, because there is a unique relationship between $S(p)$ and the deuteron energy distribution in the PWIA picture, without any additional assumptions. The fact that our calculation severely underpredicts the observed deuteron rate can be interpreted as a first hint for additional mechanisms (such as MEC) contributing to the high energy part of the nuclear response. Clearly a fully microscopic calculation of this reaction including final-state interactions is necessary to draw any firm con-

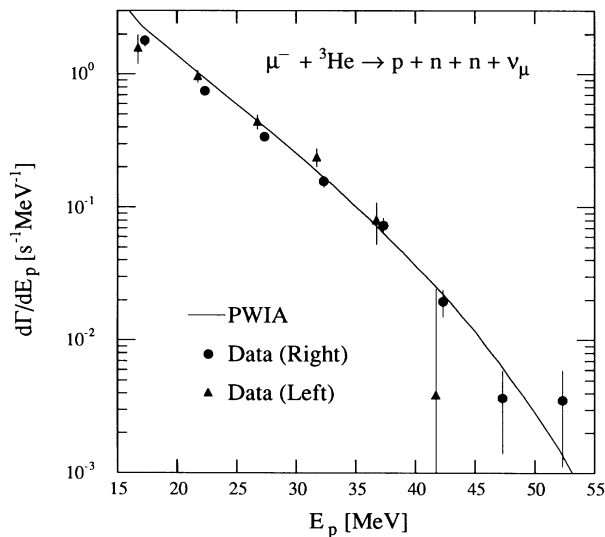


FIG. 2. The proton energy spectrum from μ^- capture by ${}^3\text{He}$. The left- and right-side data points are offset from the center of their energy bins by ± 0.3 MeV for clarity. The solid curve is the result of a PWIA calculation (see text) averaged over the measurement bins.

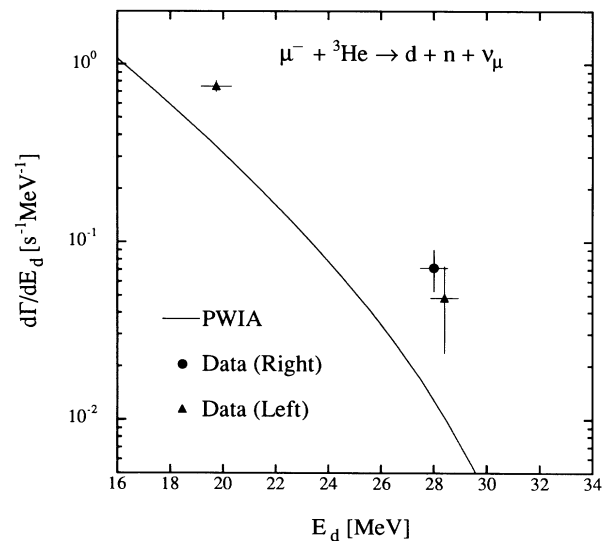


FIG. 3. The deuteron energy spectrum from μ^- capture by ${}^3\text{He}$. The horizontal error bars represent the error in the determination of the centroids of the energy bins. The solid curve is the result of a PWIA calculation (see text).

clusions. It is hoped that the existence of our data will prompt such a calculation.

We wish to thank C. J. Martoff, N. C. Mukhopadhyay, H. W. Fearing, and J. G. Congleton for valuable discussions. We gratefully acknowledge the Pew Foundation for providing the computer facility used in the analysis of this work. We also thank the entire staff at TRIUMF, particularly W. Kellner and D. C. Healey, for their generous help in carrying out the experiment. The research was supported in part by the U.S. National Science Foundation and the Natural Sciences and Engineering Research Council of Canada (NSERC).

^(a)To whom correspondence should be addressed.

- [1] M. Eckhause, R. T. Siegel, R. E. Welsh, and T. A. Filip-pas, Nucl. Phys. **81**, 575 (1966).
- [2] T. Suzuki, D. F. Measday, and J. P. Roalsvig, Phys. Rev. C **35**, 2212 (1987).
- [3] N. C. Mukhopadhyay, Phys. Rep. C **30**, 1 (1977).
- [4] H. Ullrich, in *Nuclear Physics*, Springer Tracts in Modern Physics Vol. 71 (Springer, Berlin, 1974), p. 31.
- [5] P. Singer, in *Nuclear Physics* (Ref. [4]), p. 39; Y. A. Bat-usov and R. A. Eramzhyan, Fiz. El. Chast. Atom. Yad. **8**, 229 (1977) [Sov. J. Part. Nucl. **8**, 95 (1977)].
- [6] J. van der Pluym, T. Kozlowski, W. H. A. Hesselink, A. van der Schaaf, Ch. Grab, E. A. Hermes, and W. Bertl, Phys. Lett. B **177**, 21 (1986); A. van der Schaaf, E. A. Hermes, R. J. Powers, F. D. Schleputz, R. G. Winter, A. Zgliniski, T. Kozlowski, W. Bertl, F. Felawka, W. H. A. Hesselink, and J. van der Pluym, Nucl. Phys. **A408**, 573 (1983); T. Kozlowski, W. Bertl, H. P. Povel, U. Sennhauser, H. K. Walter, A. Zgliniski, R. Engfer, Ch. Grab, E. A. Hermes, H. P. Isaak, A. van der Schaaf, J. van der Pluym, and W. H. A. Hesselink, Nucl. Phys. **A436**, 717 (1985).
- [7] C. J. Martoff, W. J. Cummings, D. Počanič, S. S. Hanna, H. Ullrich, M. Furić, T. Petković, T. Kozlowski, and J. P. Perroud, Phys. Rev. C **43**, 1106 (1991).
- [8] M. Lifshitz and P. Singer, Nucl. Phys. **A476**, 684 (1988).
- [9] M. Doi, T. Sato, H. Ohtsubo, and M. Morita, Nucl. Phys. **A511**, 507 (1990).
- [10] B. Goulard, B. Lazaro, and H. Primakoff, Phys. Rev. C **26**, 1237 (1982).
- [11] Y. K. Lee, T. J. Hallman, L. Madansky, S. Trentalange, G. R. Mason, A. J. Caffrey, E. K. McIntyre, Jr., and T. R. King, Phys. Lett. B **188**, 33 (1987).
- [12] W. Glöckle, H. Witala, and Th. Cornelius, Nucl. Phys. **A508**, 115c (1990).
- [13] E. Jans, M. Bernheim, M. K. Brussel, G. P. Capitani, E. De Sanctis, S. Frullani, F. Garibaldi, J. Morgenstern, J. Mougey, I. Sick, and S. Turck-Chieze, Nucl. Phys. **A475**, 687 (1987).